

Review Article

A Survey of Modelling and Identification of Quadrotor Robot

Xiaodong Zhang,¹ Xiaoli Li,² Kang Wang,² and Yanjun Lu¹

¹ School of Automation, Shenyang Aerospace University, Shenyang 110136, China

² School of Automation and Electrical Engineering, University of Science and Technology Beijing, Beijing 100083, China

Correspondence should be addressed to Xiaoli Li; lixiaoli@hotmail.com

Received 29 April 2014; Accepted 7 September 2014; Published 20 October 2014

Academic Editor: Shen Yin

Copyright © 2014 Xiaodong Zhang et al. This is an open access article distributed under the Creative Commons Attribution License, which permits unrestricted use, distribution, and reproduction in any medium, provided the original work is properly cited.

A quadrotor is a rotorcraft capable of hover, forward flight, and VTOL and is emerging as a fundamental research and application platform at present with flexibility, adaptability, and ease of construction. Since a quadrotor is basically considered an unstable system with the characteristics of dynamics such as being intensively nonlinear, multivariable, strongly coupled, and underactuated, a precise and practical model is critical to control the vehicle which seems to be simple to operate. As a rotorcraft, the dynamics of a quadrotor is mainly dominated by the complicated aerodynamic effects of the rotors. This paper gives a tutorial of the platform configuration, methodology of modeling, comprehensive nonlinear model, the aerodynamic effects, and model identification for a quadrotor.

1. Introduction

A quadrotor is agile to attain the full range of motion propelled by four rotors symmetrically across its center with smaller dimension and simple fabrication, unlike a conventional helicopter with complicated mechanism. Generally, it should be classified as a rotary-wing aircraft according to its capability of hover, horizontal flight, and vertical take-off and landing (VTOL) [1]. In 1920s, the prototypes of manned quadrotors were introduced for the first time [1, 2]; however, the development of this new type of air vehicle is interrupted for several decades due to various reasons such as mechanical complexity, large size and weight, and difficulties in control especially. Only in recent years a great deal of interests and efforts have been attracted on it; a quadrotor has even become a more optional vehicle for practical application, such as search-and-rescue and emergency response amazingly. As a small, unmanned aerial vehicle (UAV), it has versatile forms from 0.3 to 4 kg. Up to now, some large quadrotors already have sufficient payload and flight endurance to undertake a number of indoor and outdoor applications, like Bell Boeing Quad TiltRotor and so forth [3]. With the improvements of high energy lithium battery, MEMS sensor and other technologies, especially, the scope for commercial opportunities is

rapidly increasing [4]. As a quadrotor is inexpensive and easy to be designed and assembled, as well as the complex dynamics, such a rotorcraft is emerging as a fundamental research platform for aerial robotics research for the problems related to three-dimensional mobility and perception [5]. Furthermore, a quadrotor's design and implementation have even become a Multidisciplinary Engineering Undergraduate Course nowadays for the aim to teach students to cope with the challenges, for instance, fast and unstable dynamics and tight integration of control electronics and sensors [6].

For the specific purposes including academic research, commercial usage, and even military aim, many research groups or institutions have fabricated various quadrotors, such as the X4-flyer [7], OS4 [8], STARMAC [9], and Pixhawk [10] which have become the shining stars mentioned on the network, magazines, and all kinds of academic journals. It is worthy to note that the Draganflyer X4, Asctec Hummingbird, Gaii Quad flyer, and DJI Wookong have been introduced and developed in the comprehensive commercial market. For the powerful operation, some new types of quadrotors with tilting propellers or a new configuration, have been constructed in [10–15] in order to address the issues such as underactuated system. In addition, a number of OSPs (open-source projects) for quadrotors have emerged

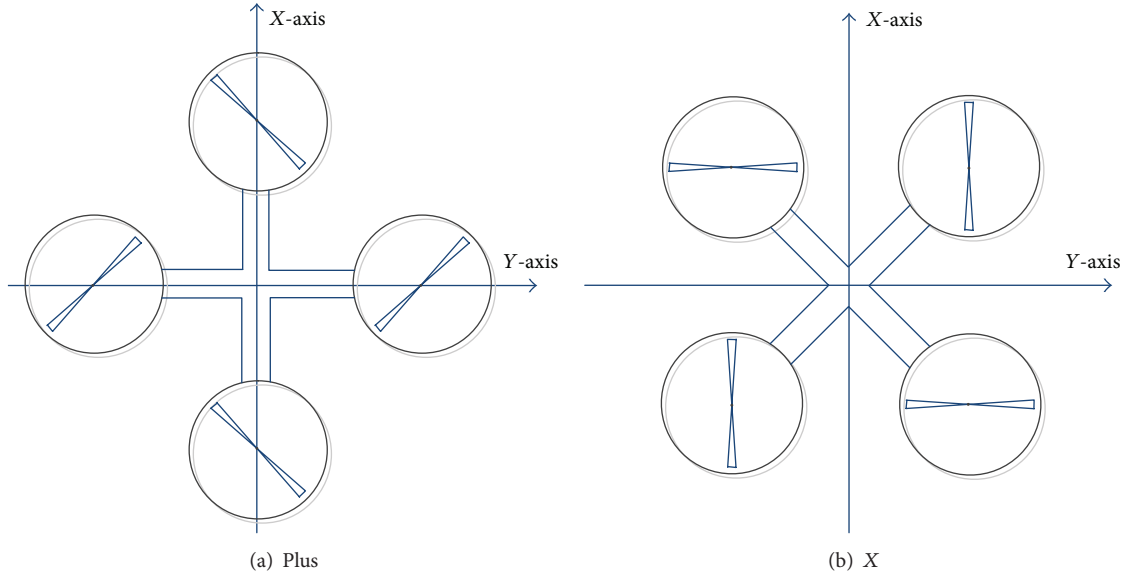


FIGURE 1: Plus and X quadrotor configurations.

with contributions from RC hobbyists, universities, and corporations [16].

A quadrotor helicopter is a highly nonlinear, multi-variable, strongly coupled, underactuated, and basically an unstable system (6 DOF with only 4 actuators), which acts as preliminary foundation for design of control strategy. Many controllers have been presented to overcome the complexity of the control resulting from the variable nature of the aerodynamic forces in different conditions of flight [17]. Many works have been published on control issues about quadrotors, such as PID controllers [18–21], linear quadratic LQR algorithm [22, 23], H_∞ loop forming method [24], sliding mode variable structure control, feedback linearization [25, 26], backstepping [27, 28], and even intelligent control [29, 30]. In those works above, the linearization of the nonlinear model around hover flight regime is conducted and used to construct controller to stabilize the quadrotor's attitude under small roll and pitch angles. The treatments to the vehicle dynamics, based on some simplistic assumptions, have often ignored known aerodynamic effects of rotorcraft vehicles. In the case of hovering and forward flight with slow velocity, those assumptions are approximately reasonable.

As the quadrotor research shifts to new research areas (i.e., mobile manipulation, aerobatic moves, etc.) [31, 32], the need for an elaborate mathematical model arises, and the simplistic assumption is no more suitable. When aggressive maneuvers such as fast forward and heave flight actions, VTOL, and the ground effect appear, the dynamics of quadrotors could be influenced significantly under these aerodynamic force and moment. It is shown in [33] that existing techniques of modeling and control are inadequate for accurate trajectory tracking at higher speed and in uncertain environments if aerodynamic influence is ignored. The model incorporated with a full spectrum of aerodynamic effects that impact on the quadrotor in faster climb, heave, and forward flight has become an area of active research

with considerable effort focusing on strategies for generating sequences of controllers to stabilize the robot to a desired state.

Traditionally, first principle assumptions and measurements of vehicle parameters can be used to derive nonlinear models, from which linear models can be obtained. As an alternative, system identification is also powerful to derive dynamic models directly from flight test data to overcome the challenges such as hardly obtained parameters of the underlying physics of the vehicle. Even though there exists a large volume of multirotor research, there is very little research into system ID of multirotors [34]. The reason for this absence is partially due to the unstable system dynamics of the quadrotor, which makes open-loop identification nonpractical.

This paper provides a tutorial introduction to configuration, modeling, aerodynamics effects analysis, and model identification for quadrotor. The paper's basic structure is as follows: above all, the characteristics and configuration of quadrotor are introduced, then two formulations for the model of quadrotor are compared, and a comprehensive nonlinear equation characterizing the dynamics of quadrotor is derived. Thereupon, aerodynamic effects that impact on the quadrotor in aggressive maneuvers are revealed. At last, several methods about identification are reviewed.

2. Characteristics of Quadrotor

Typically, the structure of a quadrotor is simple enough, which comprises four rotors attached at the ends of arms under a symmetric frame. The dominating forces and moments acting on the quadrotor are given by rotors driven with motors, especially BLDC motors. According to the orientation of the blades, relative to the body coordinate system, there are two basic types of quadrotor configurations: plus and cross-configurations shown in Figure 1.

In the plus configuration selected by most of the quadrotors, a pair of blades, spinning in the same clockwise or counter-clockwise direction, are fabricated on x and y coordinates of the body frame coordinate system, such as the assemble of the Draganflyer XPro. On the contrary, a different cross-configuration is adopted by some other quadrotors, such as the Convertawings model A, the Piasecki PA-39, or the Curtiss-Wright VZ-7AP, in which there is no rotor at the front or the rear but instead two rotors are on the right side and two on the left.

In contrast with the plus configuration, for the same desired motion, the cross-style provides higher momentum which can increase the maneuverability performance as each move requires all four blades to vary their rotation speed [35]. However, the attitude control is basically analogous [36].

It is the configuration of a quadrotor that shows the inherent characteristics. Basic control sequences of cross-configuration are shown in Figure 2. The quadrotor's translational motion depends on the tilting of rotorcraft platform towards the desired orientation. Hence, it should be noted that the translational and rotational motion are tightly coupled because the change of rotating speed of one rotor causes a motion in three degrees of freedom. This is the reason that allows the quadrotor with six degrees of freedom (DOF) to be controlled by four inputs; therefore the quadrotor is an underactuated system.

In principle, a quadrotor is dynamically unstable and therefore proper control is necessary to make it stable. Despite of unstable dynamics, it is good for agility. The instability comes from the changing rotorcraft parameters and the environmental disturbances such as wind [37]. In addition, the lack of damping and the cross-coupling between degrees of freedom make it very sensitive to disturbances.

3. 6-DOF Airframe Dynamics

Dominating methods as Euler-Lagrange formalism and Newton-Euler formalism are applied to model the dynamics for an aircraft [38–44]. It has been noted that the Newton-Euler method is easy to be understood and accepted physically despite of the compact formulation and generalization shown by Euler-Lagrange formalism. Nevertheless, two methods are consistent for the description of dynamics. That is to say, it is indicated that after a speed transform matrix the Lagrange equation is an expression form of the second Newton Law [45].

3.1. Euler-Lagrange Formalism. The generalized coordinates of the rotorcraft are given in [46]:

$$\mathbf{q} = (x, y, z, \psi, \theta, \phi) \in R^6, \quad (1)$$

where $(x, y, z) = \boldsymbol{\xi} \in R^3$ denotes the position of the mass center of the quadrotor relative to the inertial frame and $(\psi, \theta, \phi) = \boldsymbol{\eta} \in R^3$ are the three Euler angles (resp., yaw, pitch, and roll), under the conditions $(-\pi \leq \psi \leq \pi)$ for yaw, $(-\pi/2 \leq \theta \leq \pi/2)$ for pitch, and $(-\pi/2 \leq \phi \leq \pi/2)$ for roll, which represent the orientation of the rotorcraft (see Figure 3).

Naturally, translational and rotational coordinates are obtained from the model

$$\boldsymbol{\xi} = (x, y, z) \in R^3, \quad \boldsymbol{\eta} = (\psi, \theta, \phi) \in R^3. \quad (2)$$

The translational and the rotational kinetic energy of the rotorcraft are

$$T_{\text{trans}} \triangleq \frac{m}{2} \dot{\boldsymbol{\xi}}^T \dot{\boldsymbol{\xi}}, \quad T_{\text{rot}} \triangleq \frac{1}{2} \dot{\boldsymbol{\eta}}^T J \dot{\boldsymbol{\eta}}, \quad (3)$$

where m denotes the mass of the quadrotor. $J = \mathbf{W}^T I \mathbf{W}$ is the moment of inertia matrix in the inertial coordinate system after being transformed from the body frame, by matrix \mathbf{W} :

$$\mathbf{W} = \begin{bmatrix} -\sin(\theta) & 0 & 1 \\ \cos(\theta) \sin(\psi) & \cos(\psi) & 0 \\ \cos(\theta) \cos(\psi) & -\sin(\psi) & 0 \end{bmatrix}. \quad (4)$$

The only potential energy to be considered is the gravitational potential given by $U = mgz_E$.

The Lagrangian of the rotorcraft is

$$L(\mathbf{q}, \dot{\mathbf{q}}) = T_{\text{trans}} + T_{\text{rot}} - U, \quad (5)$$

$$\dot{\boldsymbol{\xi}}^T \dot{\boldsymbol{\xi}} + \frac{1}{2} \dot{\boldsymbol{\eta}}^T J \dot{\boldsymbol{\eta}} - mgz_E = \frac{m}{2}.$$

The full rotorcraft dynamics model is derived from the Euler-Lagrange equations under external generalized forces:

$$\frac{d}{dt} \frac{\partial L}{\partial \dot{\mathbf{q}}} - \frac{\partial L}{\partial \mathbf{q}} = (F_{\boldsymbol{\xi}}, \boldsymbol{\tau}), \quad (6)$$

where $F_{\boldsymbol{\xi}} = R\hat{F}$ is the translational force applied to the quadrotor due to the throttle control input, $\boldsymbol{\tau} \in R^3$ represents the pitch, roll, and yaw moments and R denotes the rotational matrix $R(\psi, \theta, \phi) \in \text{SO}(3)$, which represents the orientation of the rotorcraft relative to a fixed inertial frame.

Since the Lagrangian contains no cross-terms in the kinetic energy combining $\dot{\boldsymbol{\xi}}$ and $\dot{\boldsymbol{\eta}}$, the Euler-Lagrange equation partitions into two parts. One obtains

$$m\ddot{\boldsymbol{\xi}} + \begin{pmatrix} 0 \\ 0 \\ mg \end{pmatrix} = F_{\boldsymbol{\xi}}, \quad (7)$$

$$J\ddot{\boldsymbol{\eta}} + \dot{J}\dot{\boldsymbol{\eta}} - \frac{1}{2} \frac{\partial}{\partial \boldsymbol{\eta}} (\dot{\boldsymbol{\eta}}^T J \dot{\boldsymbol{\eta}}) = \boldsymbol{\tau}. \quad (8)$$

Rewrite (8) as

$$J\ddot{\boldsymbol{\eta}} + C(\boldsymbol{\eta}, \dot{\boldsymbol{\eta}}) \dot{\boldsymbol{\eta}} = \boldsymbol{\tau}, \quad (9)$$

where $C(\boldsymbol{\eta}, \dot{\boldsymbol{\eta}})$ is referred to as the Coriolis terms and contains the gyroscopic and centrifugal terms.

3.2. Newton-Euler Formalism. Typically, it is necessary to define two frames of reference, each with its defined right-handed coordinate system, as shown in Figure 3. X , Y , and Z are orthogonal axes of the body-fixed frame with its

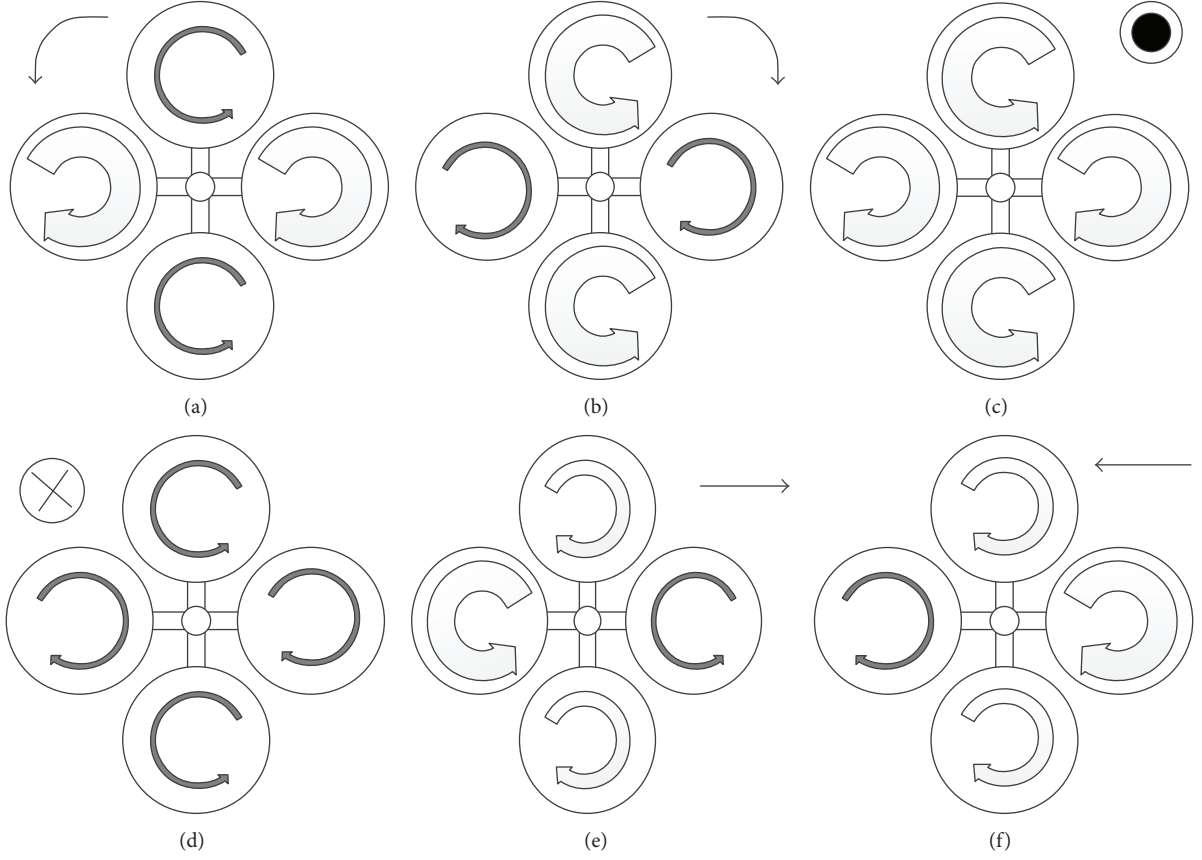


FIGURE 2: Quadrotor dynamics: (a) and (b) difference in torque to manipulate the yaw angle (Ψ); (c) and (d) hovering motion and vertical propulsion due to balanced torques; (e) and (f) difference in thrust to manipulate the pitch angle (θ) and the roll angle (ϕ).

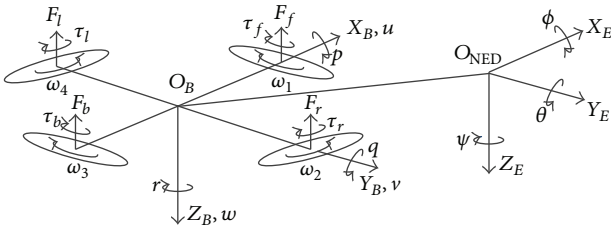


FIGURE 3: Quadrotor's body-fixed and inertial coordinate systems.

correspondent body linear velocity vector $\vec{V} = [u \ v \ \omega]^T$ and angular rate vector $\vec{\Omega} = [p \ q \ r]^T$. Another one is an Earth-fixed inertial (also known as navigation) coordinate system $E = (X_E, Y_E, Z_E)$ with which initially the body-fixed coincides. The attitude of the quadrotor, expressed in terms of the Euler angles ϕ (roll), θ (pitch), and ψ (yaw), is evaluated via sequent rotations around each one of the inertial axes. Herein, a reference frame by O_{NED} (North-East-Down) denotes an inertial reference frame and O_B a body-fixed reference frame.

Generally, a quadrotor is considered as a rigid body in a three-dimensional space. The motion equations of a quadrotor subject to external force $F \in R^3$ and torque $\tau \in$

R^3 are given by the following Newton-Euler equations with respect to the body coordinate frame $B = (X_B, Y_B, Z_B)$:

$$\begin{bmatrix} mI_{3 \times 3} & 0 \\ 0 & I \end{bmatrix} \begin{bmatrix} \dot{V} \\ \dot{\omega} \end{bmatrix} + \begin{bmatrix} \omega \times mV \\ \omega \times I\omega \end{bmatrix} = \begin{bmatrix} F \\ \tau \end{bmatrix}. \quad (10)$$

The rotorcraft orientation in space is presented by a rotation R from B to E , where $R \in SO3$ is the rotation matrix. Here c_θ is for $\cos(\theta)$ and s_θ is for $\sin(\theta)$:

$$R = \begin{pmatrix} c_\psi c_\theta & s_\phi s_\theta c_\psi - c_\phi s_\psi & c_\phi s_\theta c_\psi + s_\phi s_\psi \\ s_\theta s_\psi & s_\phi s_\theta s_\psi + c_\theta c_\psi & c_\phi s_\theta s_\psi \\ -s_\theta & s_\phi c_\theta & c_\phi c_\theta \end{pmatrix}. \quad (11)$$

With the transformation R , the first equation assessing the translational dynamics in (11) can be written in E :

$$m\ddot{\xi} = RF - mgZ_E. \quad (12)$$

Recall the kinematic relationship between the generalized velocities $\dot{\eta} = (\dot{\phi}, \dot{\theta}, \dot{\psi})$ and the angular velocity $\Omega = W\dot{\eta}$, $W \in R^{3 \times 3}$.

Defining a pseudoinertia matrix $I(\eta) = JW$ and a Coriolis vector $C(\dot{\eta}, \eta) = I\dot{\eta} + W\dot{\eta} \times I\dot{\eta}$, one can obtain

$$m\ddot{\xi} = RF - mgZ_E, \quad (13)$$

$$I(\eta)\ddot{\eta} + C(\dot{\eta}, \eta) = \tau.$$

This model has the same structure as the one obtained by the Euler-Lagrange approach, in which the main difference is the expressions of I and C , which are more complex and more difficult to implement and to compute in the case of the Euler-Lagrange method. It is important to note that the model (13) is common for all aerial robots with six degrees of freedom.

4. Basic Dynamic Model of a Quadrotor

This section introduces the basic quadrotor dynamic modeling with rigid body dynamics and kinematics. This model, based on the first order approximation, has been successfully utilized in various quadrotor control designs so far.

In the first place, some assumptions are reasonable and essential shown as follows [44].

- (i) The structure is supposedly rigid.
- (ii) The structure is supposedly symmetrical.
- (iii) The CoG (center of gravity) and the body fixed frame origin are assumed to coincide.

4.1. Dynamic Model of a Quadrotor. As we know, Newton second law is applied to the translational motion in inertial frames [47]. From the equation of Coriolis, one can obtain

$$m \frac{d\mathbf{v}}{dt_i} = m \left(\frac{d\mathbf{v}}{dt_b} + \boldsymbol{\omega}_{b/i} \times \mathbf{v} \right) = \mathbf{f}, \quad (14)$$

where m is the mass of the quadrotor, $\mathbf{f}^b \triangleq (f_x \ f_y \ f_z)^T$ is the total force applied to the quadrotor, and \mathbf{v} is the translational velocity. $\boldsymbol{\omega}_{b/i}$ is the angular velocity of the airframe with respect to the inertial frame. Since the control force is computed and applied in the body coordinate system, and since $\boldsymbol{\omega}$ is measured in body coordinates, (14) is expressed in body coordinates, where $\mathbf{v}^b \triangleq (u, v, \omega)^T$ and $\mathbf{w}_{b/i}^b \triangleq (p, q, r)^T$.

For rotational motion, Newton's second law state is

$$\frac{d\mathbf{h}}{dt_i} = \frac{d\mathbf{h}}{dt_b} + \boldsymbol{\omega}_{b/i} \times \mathbf{h} = \mathbf{m}, \quad (15)$$

where \mathbf{h} is the angular momentum and \mathbf{m} is the applied torque. $\mathbf{h}^b = \mathbf{J}\mathbf{w}_{b/i}^b$; \mathbf{J} is the constant inertia matrix. The quadrotor is essentially symmetric about all three axes, which implies that $\mathbf{J} = \text{diag}(J_x, J_y, J_z)$.

Given $\mathbf{m}^b \triangleq (\tau_\phi, \tau_\theta, \tau_\psi)^T$, which denote the rolling torque, the pitching torque, and the total yawing torque, are induced by the rotor thrust and rotor drag acting on the airframe.

The six-freedom-degree model for the quadrotor kinematics and dynamics can be summarized as follows:

$$\begin{pmatrix} \dot{x} \\ \dot{y} \\ \dot{z} \end{pmatrix} = \begin{pmatrix} c_\theta c_\psi & s_\phi s_\theta c_\psi - c_\phi s_\psi & c_\phi s_\theta c_\psi + s_\phi s_\psi \\ c_\theta s_\psi & s_\phi s_\theta s_\psi + c_\phi c_\psi & c_\phi s_\theta s_\psi - s_\phi c_\psi \\ s_\theta & -s_\phi c_\theta & -c_\phi c_\theta \end{pmatrix} \begin{pmatrix} u \\ v \\ \omega \end{pmatrix},$$

$$\begin{pmatrix} \dot{u} \\ \dot{v} \\ \dot{\omega} \end{pmatrix} = \begin{pmatrix} rv - q\omega \\ p\omega - ru \\ qu - pv \end{pmatrix} + \frac{1}{m} \begin{pmatrix} f_x \\ f_y \\ f_z \end{pmatrix},$$

$$\begin{pmatrix} \dot{\phi} \\ \dot{\theta} \\ \dot{\omega} \end{pmatrix} = \begin{pmatrix} 1 & s_\phi t_\theta & c_\phi t_\theta \\ 0 & c_\phi & -s_\phi \\ 0 & s_\phi/c_\theta & c_\phi/c_\theta \end{pmatrix} \begin{pmatrix} p \\ q \\ r \end{pmatrix},$$

$$\begin{pmatrix} \dot{p} \\ \dot{q} \\ \dot{r} \end{pmatrix} = \begin{pmatrix} \frac{J_y - J_z}{J_x} qr \\ \frac{J_z - J_x}{J_y} pr \\ \frac{J_x - J_y}{J_z} pq \end{pmatrix} + \begin{pmatrix} \frac{1}{J_x} \tau_\phi \\ \frac{1}{J_y} \tau_\theta \\ \frac{1}{J_z} \tau_\psi \end{pmatrix}. \quad (16)$$

Equation (16) is a full nonlinear model for a quadrotor, in which the complex dynamics is shown obviously, such as strong nonlinearity like the multiplication between system states, intensive coupling among the variables, and the multivariable features intuitively, that imposes the difficulties on the controller design and, on the other hand, attracts great interest of research.

4.2. Forces and Moments. The forces and torques that act on the quadrotor are primarily due to gravity and the four propellers shown in Figure 3. The steady-state thrust F_i generated by a hovering rotor (i.e., a rotor that is not translating horizontally or vertically) in free air coincides with $-Z_B$ axis. The total force acting on the quadrotor is given by

$$\mathbf{F} = F_f + F_r + F_b + F_l. \quad (17)$$

The rolling torque, the pitching torque, and the total yawing torque are given by

$$\begin{aligned} \tau_\phi &= l(F_l - F_r), & \tau_\theta &= l(F_f - F_b), \\ \tau_\psi &= \tau_r + \tau_l + \tau_f + \tau_b. \end{aligned} \quad (18)$$

The gravity force acting on the center of mass is given by

$$\mathbf{f}_g^b = R^T \begin{pmatrix} 0 \\ 0 \\ mg \end{pmatrix} = \begin{pmatrix} -mgs_\theta \\ mgc_\theta s_\phi \\ mgc_\theta c_\phi \end{pmatrix}. \quad (19)$$

Equation (16) shows strong coupled dynamics [48]: the speed change of one rotor gives rise to motion in at least 3 degrees of freedom. For instance, the speed decrease of the right rotor will roll the craft to the right under the imbalance between left and right lift forces, coupled with the rotorcraft's yaw to the right due to the imbalance in torque between clockwise and counter-clockwise, so the translation changes direction toward the front.

Nevertheless, in some cases that the rotating movement is slight, the Coriolis terms qr , pr , and pq are small and can

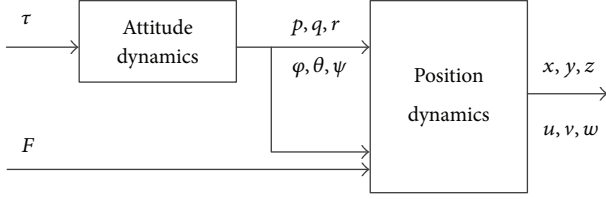


FIGURE 4: Simplified block diagram of the quadrotor's dynamics.

be neglected. So the dynamics of the quadrotor is simplified and given as [47]

$$\begin{aligned}
 \ddot{x} &= \frac{(-c_\phi s_\theta c_\psi - s_\phi s_\psi) F}{m}, \\
 \ddot{y} &= \frac{(-c_\phi s_\theta s_\psi + s_\phi c_\psi) F}{m}, \\
 \ddot{z} &= \frac{g - c_\phi c_\theta F}{m}, \\
 \ddot{\phi} &= \frac{1}{J_x} \tau_\phi, \\
 \ddot{\theta} &= \frac{1}{J_y} \tau_\theta, \\
 \ddot{\psi} &= \frac{1}{J_z} \tau_\psi.
 \end{aligned} \tag{20}$$

This model is shown in Figure 4 to which two diagrams in [49, 50] are similar. Note that the attitude of quadrotor is changed, subject to the input τ (moment) produced by each rotor. However, the position/altitude dynamics block is affected by T_j and angle variables.

Intuitively, Figure 4 gives the insight of the dynamic of the quadrotor that the angles and their time derivatives do not depend on translation components, whereas the translations depend on angle (and not on angular velocities) [50]. Based on the characteristics of the dynamics, a quadrotor control problem can be split into two distinct control problems, the inner attitude/altitude loop designed for stability and tracking of desired Euler angles and the outer X, Y, and Z position loops for regulating the vehicle position [27].

State space equations are applied in the control design and system identification generally. Hence, the nonlinear system of a quadrotor is illustrated as the formulation, which is described in different manner in [3, 27, 51]:

$$\dot{x} = f(x) + g(x)U, \tag{21}$$

where

$$\begin{aligned}
 x &= [x, y, z, \psi, \theta, \phi, u, v, \omega, p, q, r]^T, \\
 y &= [x, y, z, \psi]^T, \\
 U &= [F, \tau_\phi, \tau_\theta, \tau_\psi]^T.
 \end{aligned} \tag{22}$$

Herein the output y is composed of x, y, z and ψ is for the trajectory track, but if for the hovering control, $y = [\phi, \theta, \psi, Z]^T$ should be selected because in translation movement shown in (22), the three state variables, x, y , and z , are subordinated to the same control parameter F ; hence only one state is controllable and the others are subjected to the controlled translation and angular motions.

4.3. Gyroscopic Torques. At the normal attitude, namely, Euler angles are zero and the axes of the rotors with higher speeds spinning are coincident with the z_B axis of the robot frame. However, while the quadrotor rolls or pitches, the direction of the angular momentum vectors of the four motors is forced to be changed. A gyroscopic torque will be imposed on the airframe that attempts to turn the spinning axis so that it aligns with the precession axis. It is noted that no gyroscopic torque occurs with rotation around the z_B axis (yaw) because the spin and precession axes are already parallel [52].

The gyroscopic (inertial) moment is modeled in [53] as

$${}^b_G \vec{M}_J = \sum_{i=1}^4 J_r \left(\omega_{b/i} \times \begin{bmatrix} 0 \\ 0 \\ 1 \end{bmatrix} \right) \Omega_i, \tag{23}$$

where \vec{J}_r is the gyroscopic inertia, namely, that of the rotating part of the rotor and Ω_i is the angular rate of the rotor i ($i = 1, 2, 3, 4$).

4.4. Quaternion Differential Equations. A problem, so called gimbal lock, will appear with the Euler angle θ close to $\theta = 90^\circ$, and then the Roll angle ϕ loses its meaning. To overcome this problem, the quaternion method, which offers a mathematical notation that allows the representation of three-dimensional rotations of objects in 4D space, is selected to be the alternative remedy. Reference [54] gives a quaternion dynamics description and [55] proposes a new quaternion-based feedback control scheme for the attitude stabilization of a quadrotor aircraft.

In fact, every parameterization fails to fully represent rigid body pose in every case. That is to say, Euler angles cannot globally represent rigid body pose owing to the gimbal lock, whereas quaternions cannot define it uniquely [56]. Although researchers proved the effectiveness of using quaternions to describe aircraft dynamics, Euler angles are still the most common way of representing rigid body pose.

4.5. Linearized Model. The full nonlinear model is very useful, as it provides insight into the behavior of the vehicle. However, a linear model is used widely, which attributes to the abundance of well-studied tools available for the control system design. As we can see, most of the controllers are based on the nonlinear model with hover conditions and are stable and effective only around reasonably small angles.

Typically, the linearization of a nonlinear state space model $\dot{x} = f(x) + g(x)U$ is executed at an equilibrium point of the model

$$(x^*, U^*) : f(x^*) + g(x^*)U^* = 0. \tag{24}$$

Then, the linear model is derived by

$$A = \frac{\partial f}{\partial x} \big|_{x=x^*}, \quad B = g(x^*). \quad (25)$$

As the hovering is one of the most important regimes for a quadrotor, at this point, the condition of equilibrium of the quadrotor in terms of (24)-(25) is given as in [54]:

$$(U^*, x^*) : \begin{aligned} U_1^* &= mg \\ U_{2,3,4}^* &= 0 \\ x_{3,5,6,7,8,9,10,11}^* &= 0 \\ x_{1,2,4,12}^* &= \text{random constant.} \end{aligned} \quad (26)$$

While hovering, some assumptions are reasonable, such as the negligible influence of external forces and moments on the aircraft and small velocities and rotational velocities. By performing a Taylor series expansion and eliminating the higher order terms on (20), and using small angle approximations, a linear model is given [38, 57–59]:

$$\begin{aligned} \dot{\phi} &= p \\ \dot{\theta} &= q, \\ \dot{\psi} &= r, \\ \dot{u} &= -g\theta, \\ \dot{v} &= g\phi, \\ \dot{w} &= g - \frac{F}{m}, \\ I_{xx}\dot{p} &= \tau_\phi, \\ I_{yy}\dot{q} &= \tau_\theta, \\ I_{zz}\dot{r} &= \tau_\psi. \end{aligned} \quad (27)$$

Then the state vector is $\vec{x} = [u, v, w, p, q, r, \phi, \theta, \psi]^T$. Here, the deviations from the trim value act as the states to be considered, and all further references to aircraft states are understood to refer to the perturbation states.

Distinctly different to the linearization at hovering regime, [60] presents a new scheme, which has never before been considered in quadrotor control, in which the linearizations at four points of equilibria are conducted. The four linearizations represent different operating modes in a quadrotor flight mission. These operating modes are

- (i) hover;
- (ii) vertical motion with a constant velocity;
- (iii) horizontal translation with a constant pitch angle tilt;
- (iv) horizontal translation with a constant roll angle tilt.

All four linearizations produce four linear time-invariant systems and four controllers accordingly that are simple, low-order, and decentralized and have integral-action designed for the system stabilization despite of the issues of controller switch between two linear systems.

5. Aerodynamic Effects

In most of research projects, quadrotor dynamics has often ignored known aerodynamic effects of rotorcraft vehicles because only the stability while hovering is the aim, as stated before. At slow velocities, such as while hovering, this is indeed a reasonable assumption [61]. However, in case of demanding flight trajectories, such as fast forward and descent flight manoeuvres, as well as in the presence of the In Ground Effect, these aerodynamic phenomena could significantly influence quadrotor's dynamics [33], and the performance of control will be diminished if aerodynamic effects are not considered [62], especially in situations where the aircraft is operating at its limits (i.e., carrying heavy load, single engine breakdown, etc.).

Acting as a propulsion system, the aerodynamics of rotors plays the most important role on the movement of the quadrotor excepted with gravity and air drag with respect to the airframe. The kinematics and dynamics of the rotors are fairly complex, resulting from the combination of several types of motion, such as rotation, flapping, feathering, and lagging; normally the last two items are neglectable [3, 4]. The theoretical models based on the blade element theory (BET) combined with momentum theory (MT) show many advantages such as more flexible, more simple, and convenient in contrast with the empirical models based on empirical data typically obtained in the wind tunnel.

Note that the application of helicopter theory to a quadrotor is not straightforward for the reason of many important differences between conventional helicopter and quadrotor [1]. In order to address the issues, the specific research, with the aim at a quadrotor vehicle, is necessary to establish full model with complex dynamics subject to aerodynamic forces and moments. Many works [33, 40, 62–66] on rotor model have been done based on the results obtained for conventional helicopters [67].

Blade flapping is of significant importance in understanding the natural stability of quadrotors [4]. Since it induces forces in the x - y rotor plane of the quadrotor, the underactuated directions in the dynamics, high gain control cannot easily be implemented against the induced forces. On the other hand, the total thrust variation owing to the vertical maneuver also imposes nonignorable influence on the quadrotor behavior.

5.1. Total Thrust. In case of simplifications in aerodynamic effects, the assumption that a rotor's thrust is proportional to the square of its angular velocity is the most common consideration. However, it is proved that this assumption about rotor's thrust is especially far from reality in the cases of nonhovering regime.

The helicopter literatures [67–69] give analysis about many effects on the total thrust in more detail, in which translation lift and change of angle of attack act as the two related effects. As a rotorcraft flights across translation, the momentum of the airstream induces an increase in lift force, which is known as translational lift. The angle of attack (AOA) of the rotor with respect to the free-stream also influences

the lift, with an increase in AOA increasing thrust, just like in aircraft wings.

Applying blade element theory to quadrotor construction, the expression for rotor thrust T is given in [56]:

$$T = \frac{N\rho ac R^3 \Omega^2}{4} \left[\left(\frac{2}{3} + \mu^2 \right) \Theta_0 - (1 + \mu^2) \frac{\Theta_{tw}}{2} - \lambda_i - \lambda_c \right] \quad (28)$$

and a thrust coefficient C_T is given in

$$C_T = \left(\frac{2}{3} + \mu^2 \right) \Theta_0 - (1 + \mu^2) \frac{\Theta_{tw}}{2} - \lambda_i - \lambda_c, \quad (29)$$

where μ , λ_i , and λ_c are speed coefficients $V_{xy}/R\Omega$, $V_z/R\Omega$, and $v_i/R\Omega$, respectively. V_{xy} and V_z are the horizontal and vertical components of the total air stream velocity, respectively, and v_i is the induced velocity, and Ω is rotor angular speed. Herein, the other parameters and coefficients in the formulation above will not be described and refer to the literature [56].

Especially at hovering regime, $\mu = 0$ and $\lambda_c = 0$ (i.e., static conditions) yield

$$T = \frac{1}{2} \rho a \bar{c} R^3 (\Theta_{3/4} - \lambda_i) \Omega^2. \quad (30)$$

So one can obtain $T \propto \Omega^2$ just like the relationship between T and Ω used in the upwards context.

For the calculation of the aerodynamic coefficient C_T it is crucial to know three airspeed coefficients μ , λ_c , and λ_i . Two of them, μ , λ_c , can easily be obtained from the available motion data V_{xy} , V_z , and ΩR . λ_i however is very hard to know, because it is impossible to measure the induced velocity v_i .

One can solve this problem by means of calculating the induced velocity coefficient λ_i involved in the two aerodynamic principals, momentum, and blade element theories. In view of the fact that the macroscopic momentum equation and the microscopic blade element equation give the same rotor thrust formulation:

$$\begin{aligned} T &= \frac{N\rho a \bar{c} R^3 \Omega^2}{4} \left[\left(\frac{2}{3} + \mu^2 \right) \Theta_0 - (1 + \mu^2) \frac{\Theta_{tw}}{2} - \lambda_i - \lambda_c \right] \\ &= 2\rho R^2 \pi \lambda_i \sqrt{(\lambda_c + \lambda_i)^2 + \mu^2 + \frac{\lambda_c^2}{7.67}}. \end{aligned} \quad (31)$$

The results of solving this equation can be shown in Figure 5.

The induced velocity decreases with an increase of airflow produced by quadrotor movement, which can be seen in Figure 5. Although both direction's movements in x - y plane tend to increase induced velocity, only the vertical movement decreases the thrust coefficient. As a result, during takeoff the quadrotor loses rotor thrust, but during horizontal movement that same thrust is increased and enables more aggressive maneuvers [62, 70].

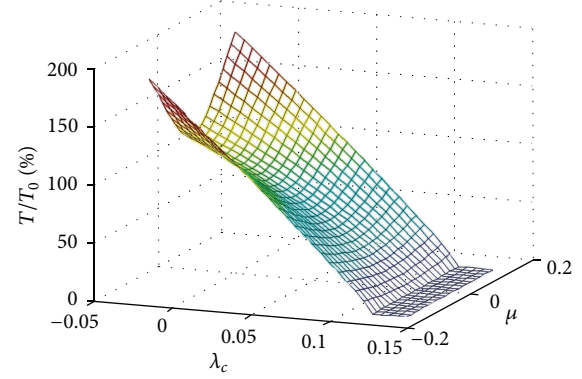


FIGURE 5: T/T_0 ratio during x - y plane movement [61].

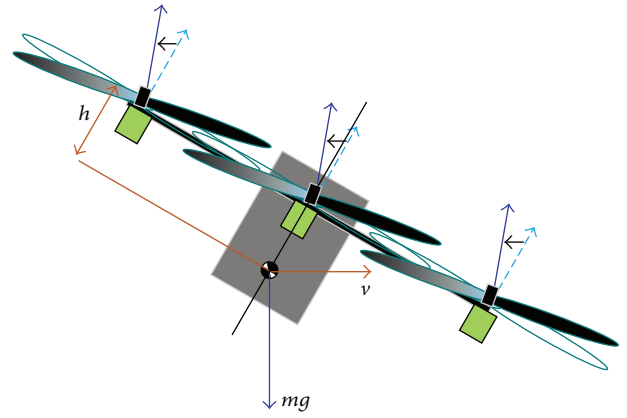


FIGURE 6: Effect of blade flapping [33].

5.2. Blade Flapping. When a rotor translates horizontally through the air, the advancing blade of the rotor has a higher velocity relative to the free-stream and will generate more lift than the retreating blade which sees a lower effective airspeed. This causes an imbalance in lift, inducing an up and down oscillation of the rotor blades, which is known as blade flapping [63, 64]. When a quadrotor is in steady state suffering the blade flapping, its rotor plane will tilt at some angle off of vertical, causing a deflection of the thrust vector illustrated in Figure 6.

In fact, the rotor thrust is perpendicular to the rotor plane and not to the hub of the rotor. Thus, in the case of blade flapping the rotor disk tilts, the rotor thrust is also inclined with respect to the airframe and imposes a component in the x and y directions of the body-fixed frame. As a result, the flapping of the blades results in a variety of effects on the dynamics of the vehicle, and in particular affecting attitude control performance [65], owing to the reason that a moment is produced for the rotor plane aligned with the vehicle's center of gravity, and the effect increases with speed.

Note that the lateral flapping was neglected in above considerations, as due to quadrotor's symmetry and in-pair counter rotation of rotors; its net influence is negligibly small in all instances of forward flight. Hence, there are two moments that need to be considered. First of all, the moment

$M_{b,lon}$ is caused by the longitudinal thrust due to a deflection angle α_{1S} between the rotor plane and rotorcraft platform:

$$M_{b,lon} = Th \sin \alpha_{1S}, \quad (32)$$

where h is the vertical distance from the rotor plane to the center of gravity of the vehicle and T is the thrust.

In addition, in the case of stiff rotors without hinges at the hub, there is also a moment $M_{b,s}$ generated directly at the rotor hub from the flapping of the blades:

$$M_{b,s} = k_\beta \alpha_{1S}, \quad (33)$$

where k_β is the stiffness of the rotor blade in Nm/rad. The total longitudinal moment created by blade flapping M_{bf} is the sum of these two moments:

$$M_{b,f} = M_{b,lon} + M_{b,s}. \quad (34)$$

Although a controller designed exactly is possibly successful to counteract small disturbances, it is difficult to reject the large systematic disturbances that result from the aerodynamic effects such as blade flapping. For the improvement of control performance, it is necessary to design a feed forward compensation block in order to cancel out moments and forces resulting from blade flapping and variations in total thrust [33].

5.3. Ground Effect and Ceiling Effect. When a rotor operates near the ground (about at half rotor diameter), a phenomenon always appears that thrust augmentation pushes the vehicle away from the ground, which is related to a reduction of the induced airflow velocity. This is called ground effect [71, 72]. Different from other approaches, an adaptive technique [73] is an option to deal with this effect. However, for the aim of improvement of the autonomous VTOL controller, a principal model of this effect is needed.

One proposed mathematical model of ground effect [74] is

$$\frac{T}{T_\infty} = \frac{1}{1 - (R/4Z)^2}. \quad (35)$$

Here R is the radius of the rotor, z is the vertical distance from the ground, T is the thrust produced by the propeller in ground effect, and T_∞ is the thrust produced at the same power outside of ground effect. Note that for $z/R = 2$ the predicted ratio between T and T_∞ is just 1.016. Therefore, this formula (35) predicts that ground effect is negligible when the rotor is more than one diameter off the ground, that is, $z/R > 2$.

Except for the ground effects, a “ceiling effect” is another issue needs to be researched, the reason is a quadrotor can flight indoor different from conventional helicopter. In fact, so called “ceiling effect” means when the vehicle is close to an overhead plane, the ceiling effect pulls the vehicle towards the ceiling which can cause a crash in the worst case. The effects have been proved by a set of experiments. Unfortunately, no formal formulation of a ceiling effect is presented so far.

6. Identification of a Quadrotor Model

Model is the foundation and the first step of control and simulation. In general, system models are derived from first principles, physical insight and sometimes input and output data, and the last two items are classified as system identification. As for a Quadrotor, the first principle scheme is intuitive to obtain the dynamical model, perhaps from the inheritance of traditional flight mechanics, by which the relationship between the inputs and outputs, that is, the underlying dynamics is revealed distinctly. However, on the other hand, the mathematical formulation proposed is characterized by the unwelcome complexity and strong nonlinearity that is regarded as a nightmare for controller design.

As a alternative solution, system identification is effective to derive a model. System identification, as the art and science of building mathematical models of dynamic systems from observed input-output data, has developed for few decades, starting from the year 1965, and enormous methods are presented. However, there are many open problems [75, 76]: such as nonlinearity and closed-loop identification, which are just the characteristics shown in the quadrotor dynamics.

Significantly, the attention on the model and identification aspect is paid on the fixed-wing and helicopter [34], instead of quadrotor, or multirotor, and the reason may be the fact of less applications of quadrotor aircraft by now, as well as relative complicated dynamics which exhibit some distinctive features on the modeling and identification schemes, presented as follows [77].

- (i) Continuous-time model is preferable. In aerospace applications, a continuous-time model looks more popular than the discrete-time one for the reason of intuition.
- (ii) To support closed-loop identification, a quadrotor system is basically open-loop unstable, so that identification experiments have to be implemented in closed loop under automatic control, or with a human operator.
- (iii) To uncouple the cross-interaction among the operation axes, the cross-coupling in dynamic behavior imposes difficulty on the estimation of a model, so that isolation of different dynamic modes is necessary to alleviate this effect.

To the best of my knowledge, although not many, some schemes dedicated to the quadrotor model identification are proposed in the following. Herein, by means of the classification in the literature [75], so called a whole palette of grey shades from white to black, these methods are introduced successively.

6.1. Off-White Models: Parameters Estimate Based on First Principle Model. A set of parameter estimates in the nonlinear quadrotor model could be taken directly from measurements, a CAD model using model software like SOLIDWORKS to model all the parts of the quadrotor, or derive from experiments, along with the associated error [66, 70,

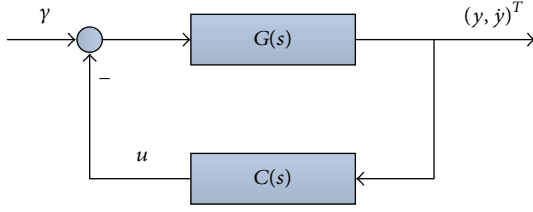


FIGURE 7: Indirect closed-loop identification setup.

78]. The parameters listed in the following context can be obtained by a regular identification method [79–81].

- (i) Aerodynamic parameters: rotor, blade, and aerodynamic parameters are obtained through measurement, computation, simulation, or from references.
- (ii) Masses and displacements: component masses and distances are measured with respect to the rotor plane.
- (iii) Rotational inertia is obtained through measurement and computation [2].
- (iv) Motor constants: resorting to some experiments conducted, the motor model can be simplified to be a first order system and the constants could be extracted from the experimental data [82, 83].

The nonlinear identification problem is to estimate such parameters from the measured data. In general, this is a difficult problem that has not yet been treated in full generality. In [84], a Levenberg-Marquardt optimization method and a quadratic optimization method are applied, respectively, to obtain the z inertia and the rotor parameters.

6.2. Steel-Grey Models: Local Linear Models Identification. Nonlinear systems are often handled by linearization around a working point. The idea behind composite local models is to deal with the nonlinearities by developing local models, which are good approximations in different neighborhoods, and then compose a global model from these. Often, the local models are linear, so a common name for composite models is also local linear models [75], as described in Section 4.5, where the hover regime is acted as a working point. After the linearization at working point, the identification issue is simplified and easy to tackle with the help of linear identification methods as follows. However, the linearization is a realistic simplification after all, which results in the bias, even model mismatch, and sometimes is unreasonable in the case of aggressive maneuvers. In addition, a set of models need to be derived in the situations that many working points exist, so the switch between two models in the model set should be paid enough attention to weaken the disturbance.

6.2.1. Parameter Identification. Using the linearized system dynamics after some treatments such as neglecting the nonlinear coupling terms, a parameter identification [85] is performed to identify separately each quadrotor axis performed in closed loop. The generic scheme of the identification process is depicted in Figure 7.

The controller $C(s)$ used during identification is a simple stabilizing, hand-tuned PD-controller with known parameters. Using linearized system dynamics equation, the identification signal, that is, a pseudorandom binary sequence (PRBS) of full length, and the controller C and output data $(y, \dot{y})^T$, one can use nonlinear optimization to estimate that our parameter vectors $\Delta_{\phi, \theta} = (p, J, T_d)^T$ and $\Delta_{\psi} = (p, z, J, T_d)^T$ are conducted, respectively. The experimental results show a very good correlation with real data, which confirms the proposed approach in which an iterative parameter identification scheme is applied, the results of which can easily be reproduced and offers great accuracy. In general, a regular procedure is implemented for the parameter identification, in which a linear model is derived from the nonlinear one with some simplification and neglecting, and then a parameter identification problem is shown, at last a iterative algorithm is applied to obtain the estimated value of the parameters, just like what is described in this literature. Next, an adaptive controller could be designed based on the parameter identification.

6.2.2. Time Domain Identification. Reference [86] presents the estimation of a linear mathematical model for the dynamics of a quadrotor by time domain system identification.

At first, the model structure has to be determined by the begin with a large pool of potential candidate regressors, meaning states or control inputs, or some combination thereof, then calculate the potential correlation of each regressor with a state derivative using a linear least-squares method. The final step in the process is to retain those regressors which have a significant correlation with the state derivative in question. The level of correlation is determined by the user so as to capture as much of the measured behavior as possible with a minimal number of regressors. An example of such a pool of regressors is given as follows:

$$\dot{u} = X_u u + X_q q + X_\theta \theta + X_{\text{lon}} \delta_{\text{lon}}, \quad (36)$$

where the state derivative \dot{u} is linearly related to the regressors, u , q , θ , and δ_{lon} , by their corresponding parameters, X_u , X_q , X_θ , and X_{lon} . This process of regressor pool correlation is repeated for each state derivative.

After the appropriate model structure has been determined, the next step is to determine the value and error of each parameter by a linear least squares method. These values form the dynamics and control matrices, A and B . At the same time, the error values are also adjusted to account for any remaining uncharacterized behavior, known as colored residuals.

The method herein is considered as the basic algorithm in the realm of system identification, which is used to address the model identification issue of linear system. It should be noted that the method is desirable for the SISO (single input and single output) system; therefore, such characteristics as cross-coupling must be mitigated in advance.

6.2.3. Frequency-Domain Identification. A frequency-domain system identification method is used to obtain

a linear representation of the quadrotor dynamics [87]. Contrast to time domain analysis, frequency-domain identification can obtain a relative robust model with the treatment of cutting down the errors associated with bias effects and processing noise, resulting in a robust model.

In the algorithm, the frequency response data acquired is validated by evaluating its coherence, which is an indication of how well the output and input data are correlated. The definition of coherence is given as

$$\gamma_{xy}^2 = \frac{|\widehat{G}_{xy}(f)|^2}{|\widehat{G}_{xx}(f)| |\widehat{G}_{yy}(f)|}, \quad (37)$$

where $\widehat{G}_{xx}(f)$, $\widehat{G}_{yy}(f)$, and $\widehat{G}_{xy}(f)$ represent the autospectral densities of the input, output, and cross-spectral density of the input and output, respectively, and are the frequency point. A perfect correlation between input and output would result in a coherence value of unity, while poor coherence typically falls below a value of 0.6.

It might also be noted that the data must be decoupled such that the inputs provided by off-axis commands are rejected from the output on the axis of interest, after the coherence of the data is validated. The multiple single output system estimation can be expressed in (38), where \widehat{H} is the system estimation:

$$\widehat{H}(f) = \widehat{G}_{xx}^{-1}(f) \widehat{G}_{xy}(f). \quad (38)$$

In the system identification process, the transfer functions of each axis will be acquired first, followed by state space representations and complete system analysis. The single input-single output (SISO) transfer function identification cost function can be defined as

$$J = \frac{20}{n_\omega} \sum_{\omega=1}^{\omega_{n_\omega}} W_\gamma \left[W_g \left(|\widehat{T}_c| - |T| \right)^2 + W_p \left(\angle \widehat{T}_c - \angle T \right)^2 \right], \quad (39)$$

where the parameters such as n_ω , ω_1 refer to [87].

As shown in [87], based on the rational experimental setup, a frequency-domain system identification method obtains a linear representation of the quadrotor dynamics. It might also be noted that the choice of the periodic excitation signal is to minimize leakage in the computation of frequency spectra, which is still an open problem in the area.

6.2.4. Subspace Model Identification. A subspace model identification (SMI) method [77], which has been proved extremely successful in dealing with the estimation of state-space models for multiple-input multiple-output (MIMO) systems is used to the identification of a quadrotor flight dynamics. More precisely, the continuous-time predictor based subspace identification approach proposed is applied to flight data collected during dedicated identification experiments, and at hovering flight condition, a linear state-space model is derived. As an advantage over the most identification techniques, this approach is feasible for the application in a closed-loop system as the correlation between u and w , v is not required. The key ideas of the algorithm are provided in the following.

Consider the linear time-invariant continuous-time system:

$$\begin{aligned} dx(t) &= Ax(t) dt + Bu(t) dt + dw(t), \quad x(0) = x_0, \\ dz(t) &= Cx(t) dt + Du(t) dt + dv(t), \\ y(t) dt &= dz(t), \end{aligned} \quad (40)$$

where $x \in R^n$, $u \in R^m$, and $y \in R^p$ are, respectively, the state, input, and output vectors and $w \in R^n$ and $v \in R^p$ are the process and the measurement noise, respectively, modeled as Wiener processes with incremental covariance given by

$$E \left\{ \begin{bmatrix} dw(t) \\ dv(t) \end{bmatrix} \begin{bmatrix} dw(t) \\ dv(t) \end{bmatrix}^T \right\} = \begin{bmatrix} Q & S \\ S^T & R \end{bmatrix}. \quad (41)$$

The system matrices A , B , C , and D , of appropriate dimensions, are such that (A, C) is observable and $(A[B, Q^{1/2}],)$ is controllable. Assume that a data set $u(t_i)$, $y(t_i)$, $i[1, N]$ of sampled input/output data obtained from (41) is available. Then, the problem is to provide a consistent estimate of the state space matrices A , B , C , and D on the basis of the available data.

Note that both model order and the tuning parameters of the identification algorithm (i.e., the position of the Laguerre pole a and the parameters of the **PBSID**_{opt} algorithm) need to be achieved at the head of the procedure; herein, a cross-validation approach, explained in detail in the literature [77], is used to address the issue.

As can be observed from the experiments, in which the input signal adopted for identification experiments is the so-called 3211 piecewise constant sequence, the identified models capture the essential features of the response of the quadrotor along all the axes. As it is known that the SMI method is rapid and easy to use, however, the model deserved from the algorithm is not based on some kind of optimal criteria, so the model obtained is also not believed to be optimum.

6.2.5. UKF Method. As we know, if the systems have severe nonlinearities, EKF can be hard to tune and often gives unreliable estimation due to the linearization relied by the EKF in order to propagate the mean and covariance of the states. Therefore, UKF is applied for the identification of a quadrotor model [88].

For the quadrotor system with continuous-time system dynamics,

$$\begin{aligned} \dot{x} &= Ax + Bu, \\ y &= Cx. \end{aligned} \quad (42)$$

Since the state vector of the quad-rotor

$$x_k = (x, y, z, \dot{x}, \dot{y}, \dot{z}, \phi, \theta, \psi, \dot{\phi}, \dot{\theta}, \dot{\psi})^T \quad (43)$$

the system state equation can be derived according to the full nonlinear equations. Finally, based on all of the system equations, the parameters to be estimated and identified are formulated as follows:

$$\Theta = (I_{xx}, I_{yy}, I_{zz}, I_R, \dot{x}, \dot{y}, \dot{z}, \dot{\phi}, \dot{\theta}, \dot{\psi})^T. \quad (44)$$

Based the experiments, the error of the estimation for velocity at x -axes is less than 0.001, while the errors at both y -axes and z -axes are less than 0.0015. For estimation of angular velocities at x , y , and z -axes, the errors are less than 0.0015. From the errors computed, it can be concluded that the UKF output matches with the measured output and the measured noise is well filtered by the UKF. It has good convergence time and relatively reliable for the estimations.

6.3. Slate-Grey Models: RBF-ARX Model. The RBF-ARX model is a nonlinear time-varying model whose structure resembles the ARX model. Its independent variables are groups of signals indicating the nonlinear status of the system, and its model parameters can be promptly adjusted to the best by taking the advantages of the RBF neural network. Owing to the self-adjusting parameters, the RBF-ARX model not only has an outstanding approximation in local linear space but also has superior global performance. RBF-ARX basic model structure of a quadrotor is shown as follows [89, 90]:

$$\begin{aligned}
 y(t) &= c(\omega(t)) + \sum_{k=1}^{n_y} A_k(\omega(t)) Y(t-k) \\
 &+ \sum_{k=d}^{n_u} B_k(\omega(t)) U(t-k) + e(t), \\
 C(\omega(t)) &= [\phi_0^1(\omega(t)) \phi_0^2(\omega(t)) \phi_0^3(\omega(t))]^T, \\
 \phi_0^i(\omega(t)) &= c_0^i + \sum_{m=1}^h c_m^i \exp \left\{ -\|\omega(t) - z_{Y,m}\|_{\lambda_{r,m}}^2 \right\},
 \end{aligned} \tag{45}$$

where n_y , n_u , m , and h are the order of the system, d is delay factor of system, and $e(t)$ is white noise. A quadrotor system is a nonlinear system with four inputs and 3 outputs, and the inputs are the input electric voltage of four rotors, that is, $U(t) = [V_f(t) \ V_r(t) \ V_l(t) \ V_b(t)]^T$, and the three outputs are pitch, roll, and yaw angles, respectively, that is, $Y(t) = [p(t) \ r(t) \ y(t)]^T$ and $w(t) = [p(t) \ r(t)]^T$. A set of simulation tests show that the error of RBF-ARX model is most close to a normal distribution, which indicates that the good model is obtained. In addition, no matter how the state variable $\omega(t)$ slides, the distribution of system pole does not go beyond the stable scope. So the RBF-ARX model is suitable for quadrotor.

6.4. Black Models

6.4.1. Neural Network Model. A black box model that uses a neural network to learn the dynamics of the quadrotor is attempted [79]. The nonlinear autoregressive network with exogenous inputs (NARX) architecture is setup which has 6 different nets, one each for the X , Y , and Z velocities and roll, pitch, and yaw rates. The other variables are then integrated (position/angles) and derive (accelerations) from the calculated velocities/rates. The procedure, described in Figure 8, is designed to address the issue of the current prediction

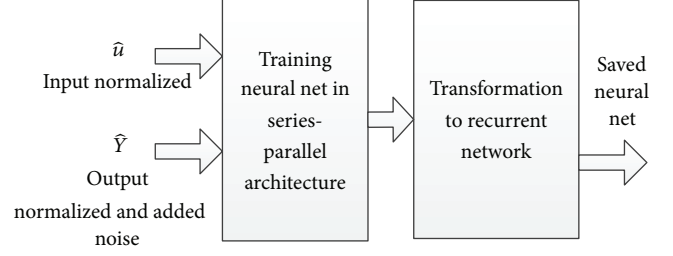


FIGURE 8: The flow for training the neural net.

(y_t) dependent on the predicted output for the previous time point (y_{t-1}), in which a series-parallel architecture, $Y(t-1)$ is the correct output for time point $t-1$, $u(t)$ is the input vector for time point t , and $y(t)$ is the prediction for time point t , is used for training before converting the net to the parallel architecture.

Some tests result shows that the black box neural network model can predict both the roll and pitch with very good accuracy and however perform not better for the yaw rate, which will be improved by creating a larger net or by adding more variables to the state vector for the nets. Surprisingly, the model was tested on a manoeuvre for which it had not been trained; a successful result is obtained. This result shows that the black box neural network model learned not only the dynamics of the quadrotor but also the dynamics of the trends and the noise. Neural networks have proved to be a remarkable modeling scheme carried out in various applications; however, on the other hand, substantial amount of tests need to be taken. Obviously, the work is costly and time-consuming.

6.4.2. Data-Based Model. The main purpose of data-based techniques is to take full advantage of the information acquired from huge amounts of process measurements. Without recourse to physical models obtained from first principles, a relatively overall perspective of system performance could be revealed via available measurements. Through deep insights of process measurements, information like system characteristics and regularity can be dug out for optimal modeling and decision making. The description [91] aforementioned reveals the insight and application of data-based model identification schemes.

It is noted that several typical data-based approaches, which only depend on process measurements, principal component analysis (PCA), partial least squares (PLS), and their variants, are successfully utilized in many areas [92–96]. In the realms of model and control, iterative learning control (ILC) scheme, and model free adaptive control (MFAC)—in essence, model free methods—show great advantages without a priori knowledge about the underlying processes, such as time delay and system order, despite their potential limit for processes with high complexity.

In addition, the recent developments on model-data integrated approaches, which also rely on available process measurements and a prior known limited knowledge about

the processes for monitoring and control purposes, the iterative feedback tuning (IFT), and virtual reference feedback tuning (VRFT), have become the promising research topics. Although there are no reports of the application of the data-based model identification on the quadrotor so far, these approaches will soon find their utilizations.

Remark. Hover condition is the main status of the quadrotor, as quite a few tasks, such as surveillance, search, and rescue, are implemented in the condition. Therefore, linear model is simplified on the complex nonlinear one derived from first principle model, in which the feasibility is proved by application result. However, aggressive maneuver shows the obvious nonlinear characteristics, so that the nonlinear model is needed, in which neural networks are an optional scheme despite the fact that a large amount of tests are indispensable. The data-based approaches have shown the distinctive advantages in other application areas; the utilization on a quadrotor will be a commendable attempt. It is noted that these methods aforementioned not only are applicable in the quadrotor aspect but also is helpful to the field with the similar characteristics, such as active suspension systems of vehicle investigated in [97, 98].

7. Conclusion and Perspective

By now, a quadrotor has been a preferable platform of aircraft design and autonomous control due to the distinct characteristics involved in the craft configuration and flight dynamics, and the expansion to the commercial and military application is underway. The research results at present show that the static and dynamic characteristics of a quadrotor have been developed, and the aerodynamic effects on the craft flight performance have been revealed with the help of the conventional rotor theory.

As a base and preliminary for the next control and simulation work, the paper surveys the state of art of the modeling and identification of a quadrotor; afterwards some opinions are given as follows.

- (1) The full nonlinear equations have been obtained by classical Euler-Newtonian mechanics as well as Lagrange equation, with the knowledge of different force imposed on, especially aerodynamic function. However, there is no specific research of the model of a quadrotor, in which the dynamics is described comprehensively and systematically.
- (2) The dynamics of quadrotor shows distinct characteristics for the VTOL, horizontal flight, aggressive maneuver, and hovering mode involved in the execution of flight task. Whereas at the present, the hovering mode attracts over much attention, probably owing to the fact that the hovering is the one of the important working modes. Obviously, more efforts of research should be paid on the other modes such as aggressive maneuver.
- (3) The method of multistatic status linearization model has been presented at the aim of control, which may be an effective way to address the issue of complex dynamics. However, a problem of undisturbed switching between the multimodels should be resolved.
- (4) In contrast with the other crafts, there is no more attention for the model identification of a quadrotor for the reason of the requirements mentioned in the paper. The effective transplantation of the identification methods used in the other respects is a practical choice.
- (5) A new configuration of quadrotor with tilt rotor can eliminate the deficiency such as underactuate feature. The relative research work has been in progress, which will be a focus hereafter.

Conflict of Interests

The authors declare that there is no conflict of interests regarding the publication of this paper.

Acknowledgments

This work was supported by the Fundamental Research Funds for the Central Universities (Grant no. FRF-TP-12-005B), Program for New Century Excellent Talents in Universities (Grant no. NCET-11-0578), Aeronautical Science Foundation of China (Grant no. 2012ZD54013), and Specialized Research Fund for the Doctoral Program of Higher Education (Grant no. 20130006110008).

References

- [1] V. Martinez, *Modeling of the flight dynamics of a quadrotor Helicopter* [M.S. thesis], Cranfield University, Cranfield, UK, 2007.
- [2] M. Y. Amir and V. Abbass, "Modeling of quadrotor helicopter dynamics," in *Proceedings of the International Conference on Smart Manufacturing Application (ICSMA '08)*, pp. 100–105, Kintex, April 2008.
- [3] G. Warwick, "US Army looking at three configuration concepts for large cargo rotorcraft," September 2013, <http://www.flightglobal.com/news/articles/us-army-looking-at-three-configuration-concepts-for-large-cargo-rotorcraft-217956/>.
- [4] R. Mahony, V. Kumar, and P. Corke, "Multirotor aerial vehicles: modeling, estimation, and control of quadrotor," *IEEE Robotics and Automation Magazine*, vol. 19, no. 3, pp. 20–32, 2012.
- [5] R. Mahony and V. Kumar, "Aerial robotics and the quadrotor," *IEEE Robotics and Automation Magazine*, vol. 19, no. 3, p. 19, 2012.
- [6] I. Gaponov and A. Razinkova, "Quadcopter design and implementation as a multidisciplinary engineering course," in *Proceedings of the 1st IEEE International Conference on Teaching, Assessment, and Learning for Engineering (TALE '12)*, pp. B16–B19, IEEE, Hong Kong, China, August 2012.
- [7] N. Guenard, T. Hamel, and R. Mahony, "A practical visual servo control for an unmanned aerial vehicle," *IEEE Transactions on Robotics*, vol. 24, no. 2, pp. 331–340, 2008.
- [8] S. Bouabdallah and R. Siegwart, "Towards intelligent miniature flying robots," in *Tractsaction in Advanced Robotics*, vol. 25, pp. 429–440, Springer, Berlin, Germany, 2006.

- [9] G. Hoffmann, D. G. Rajnarayan, S. L. Waslander, D. Dostal, J. S. Jang, and C. J. Tomlin, "The stanford testbed of autonomous rotorcraft for multi agent control (STARMAC)," in *Proceedings of the 23rd Digital Avionics Systems Conference (DASC '04)*, vol. 2, pp. 12.E.4–12.I.10, Salt Lake City, Utah, USA, October 2004.
- [10] L. Meier, P. Tanskanen, F. Fraundorfer, and M. Pollefeys, "PIXHAWK: a system for autonomous flight using onboard computer vision," in *Proceedings of the IEEE International Conference on Robotics and Automation (ICRA '11)*, pp. 2992–2997, IEEE, Shanghai, China, May 2011.
- [11] S. K. Phang, C. Cai, B. M. Chen, and T. H. Lee, "Design and mathematical modeling of a 4-standard-propeller (4SP) quadrotor," in *Proceeding of the 10th World Congress on Intelligent Control and Automation (WCICA'12)*, pp. 3270–3275, Beijing, China, July 2012.
- [12] M. S. Hossain, A. M. Kabir, and P. Mazumder, "Design and development of an Y4 Copter control system," in *Proceedings of the 14th International Conference on Computer Modeling and Simulation (UKSim'12)*, pp. 251–256, Cambridge, UK, March 2012.
- [13] F. Senkul and E. Altug, "Modeling and control of a novel tilt: roll rotor quadrotor UAV," in *Proceeding of the International Conference on Unmanned Aircraft Systems (ICUAS'13)*, pp. 1071–1076, Atlanta, Ga, USA, May 2013.
- [14] M. Ryll, H. H. Bulthoff, and P. R. Giordano, "First flight tests for a quadrotor UAV with tilting propellers," in *Proceedings of the IEEE International Conference on Robotics and Automation (ICRA '13)*, pp. 295–302, IEEE, Karlsruhe, Germany, May 2013.
- [15] S. Driessens and P. E. I. Pounds, "Towards a more efficient quadrotor configuration," in *Proceedings of the IEEE/RSJ International Conference on Intelligent Robots and Systems (IROS '13)*, pp. 1386–1392, Tokyo, Japan, 2013.
- [16] H. Lim, J. Park, D. Lee, and H. J. Kim, "Build your own quadrotor: Open-source projects on unmanned aerial vehicles," *IEEE Robotics and Automation Magazine*, vol. 19, no. 3, pp. 33–45, 2012.
- [17] D. Mellinger and V. Kumar, "Minimum snap trajectory generation and control for quadrotors," in *Proceedings of the IEEE International Conference on Robotics and Automation (ICRA '11)*, pp. 2520–2525, IEEE, Shanghai, China, May 2011.
- [18] Q. Zhan, J. Q. Wang, and X. Xi, "Control system design and experiments of a quadrotor," in *Proceedings of the IEEE International Conference on Robotics and Biomimetics (ROBIO '12)*, pp. 1152–1157, IEEE, Guangzhou, China, December 2012.
- [19] L. Jun and Y. T. Li, "Dynamic analysis and PID control for a quadrotor," in *Proceedings of the International Conference on Mechatronics and Automation*, pp. 573–578, IEEE, Beijing, China, August 2011.
- [20] A. L. Salih, M. Moghavvemi, H. A. F. Mohamed, and K. S. Gaeid, "Flight PID controller design for a UAV quadrotor," *Scientific Research and Essays*, vol. 5, no. 23, pp. 3660–3667, 2010.
- [21] A. B. Milhim, Y. Zhang, and C. A. Rabbath, "Quadrotor UAV-high fidelity modeling and nonlinear PID control," in *Proceedings of AIAA Modeling and Simulation Technologies Conference*, pp. 2010–8362, Toronto, Canada, 2010.
- [22] R. Zawiski and M. Błachuta, "Model development and optimal control of quadrotor aerial robot," in *Proceedings of the 17th International Conference on Methods and Models in Automation and Robotics (MMAR '12)*, pp. 475–480, Miedzydroje, Poland, August 2012.
- [23] E. Reyes-Valeria, R. Enriquez-Caldera, S. Camacho-Lara, and J. Guichard, "LQR control for a quadrotor using unit quaternions: modeling and simulation," in *Proceedings of the 23rd International Conference on Electronics, Communications and Computing (CONIELECOMP '13)*, pp. 172–178, IEEE, Cholula, Mexico, March 2013.
- [24] M. Rich, N. Elia, and P. Jones, "Design and implementation of an H_∞ controller for a quadrotor helicopter," in *Proceeding of the 21st Mediterranean Conference on Control and Automation (MED '13)*, pp. 1189–1198, Chania, Greece, June 2013.
- [25] P. Mukherjee and S. L. Waslander, "Direct adaptive feedback linearization for quadrotor control," in *Proceedings of the AIAA Guidance, Navigation, and Control Conference*, pp. 2012–4917, Minneapolis, Minn, USA, August 2012.
- [26] A. Khalifa, M. Fanni, A. Ramadan, and A. Abo-Ismael, "Modeling and control of a new quadrotor manipulation system," in *Proceedings of the 1st International Conference on Innovative Engineering Systems (ICIES '12)*, pp. 109–114, Alexandria, Egypt, December 2012.
- [27] L. Pollini and A. Metrangolo, "Simulation and robust backstepping control of a Quadrotor aircraft," in *Proceedings to AIAA Modeling and Simulation Technologies Conference and Exhibit*, pp. 2008–6363, Honolulu, Hawaii, USA, 2008.
- [28] A. A. Mian and D. B. Wang, "Modeling and backstepping-based nonlinear control strategy for a 6 DOF quadrotor helicopter," *Chinese Journal of Aeronautics*, vol. 21, no. 3, pp. 261–268, 2008.
- [29] F. Casolo, *Motion Control*, InTech, Croatia, Rijeka, 2010.
- [30] M. Santos, V. López, and F. Morata, "Intelligent fuzzy controller of a quadrotor," in *Proceedings of the IEEE International Conference on Intelligent Systems and Knowledge Engineering (ISKE '10)*, pp. 141–146, IEEE, Hangzhou, China, November 2010.
- [31] C. M. Korpela, T. W. Danko, and P. Y. Oh, "MM-UAV: mobile manipulating unmanned aerial vehicle," *Journal of Intelligent and Robotic Systems*, vol. 65, no. 1–4, pp. 93–101, 2012.
- [32] D. Mellinger, N. Michael, and V. Kumar, "Trajectory generation and control for precise aggressive maneuvers," *Springer Tracts-action in Advanced Robotics*, vol. 79, pp. 361–373, 2014.
- [33] H. M. Huang, G. M. Hoffmann, S. L. Waslander, and C. J. Tomlin, "Aerodynamics and control of autonomous quadrotor helicopters in aggressive maneuvering," in *Proceedings of the IEEE International Conference on Robotics and Automation (ICRA '09)*, pp. 3277–3282, IEEE, Kobe, Japan, May 2009.
- [34] N. V. Hoffer, C. Coopmans, A. M. Jensen, and Y. Q. Chen, "A survey and categorization of small low-cost unmanned aerial vehicle system identification," *Journal of Intelligent and Robotic Systems*, vol. 74, no. 1–2, pp. 129–145, 2014.
- [35] S. Gupte, P. I. T. Mohandas, and J. M. Conrad, "A survey of quadrotor unmanned aerial vehicles," in *Proceeding of the IEEE Southeastcon*, pp. 1–6, Orlando, Fla, USA, March 2012.
- [36] A. R. Partovi, A. Z. Y. Kevin, H. Lin, B. M. Chen, and G. Cai, "Development of a cross style quadrotor," in *Proceedings of the AIAA Guidance, Navigation, and Control Conference*, St. Paul, Minn, USA, August 2012.
- [37] E. Altuğ, J. P. Ostrowski, and R. Mahony, "Control of a quadrotor helicopter using visual feedback," in *Proceedings of the IEEE International Conference on Robotics and Automation*, pp. 72–77, IEEE, Washington, DC, USA, May 2002.
- [38] D. S. Miller, *Open loop system identification of a micro quadrotor helicopter from closed loop data [M.S. dissertation]*, University of Maryland, College Park, Md, USA, 2011.

- [39] J. Dvorak, *Micro quadrotor-design, modeling, identification and control [M.S. thesis]*, Czech Technical University, Prague, Czech Republic, 2011.
- [40] P. Pounds, R. Mahony, and P. Corke, "Modelling and control of a large quadrotor robot," *Control Engineering Practice*, vol. 18, no. 7, pp. 691–699, 2010.
- [41] J. H. Kim, M.-S. Kang, and S. Park, "Accurate modeling and robust hovering control for a quad-rotor VTOL aircraft," *Journal of Intelligent and Robotic Systems*, vol. 57, no. 1–4, pp. 9–26, 2010.
- [42] M. Elsamanty, A. Khalifa, M. Fanni, A. Ramadan, and A. Abo-Ismael, "Methodology for identifying quadrotor parameters, attitude estimation and control," in *Proceedings of the IEEE/ASME International Conference on Advanced Intelligent Mechatronics (AIM '13)*, pp. 1343–1348, Wollongong, Australia, July 2013.
- [43] J. Kim, M.-S. Kang, and S. Park, "Accurate modeling and robust hovering control for a quad-rotor VTOL aircraft," *Journal of Intelligent and Robotic Systems*, vol. 57, no. 1–4, pp. 9–26, 2010.
- [44] T. Bresciani, *Modelling, identification and control of a quadrotor Helicopter [M.S. thesis]*, Lund University, Lund, Sweden, 2008.
- [45] H. J. Wang, "The essence of dynamic mechanics for lagrange equation," *Journal of Hebei University of Science and Technology*, vol. 24, no. 2, pp. 56–60, 2003 (Chinese).
- [46] P. Castillo, R. Lozano, and A. Dzul, "Stabilization of a mini-robotcraft having four rotors," in *Proceedings of the IEEE/RSJ International Conference on Intelligent Robots and Systems (IROS '04)*, pp. 2693–2698, Sendai, Japan, October 2004.
- [47] R. W. Beard, *Quadrotor Dynamics and Control*, Brigham Young University, 2008.
- [48] P. McKerrow, "Modelling the draganflyer four-rotor helicopter," in *Proceedings of the IEEE International Conference on Robotics and Automation*, pp. 3596–3601, New Orleans, La, USA, May 2004.
- [49] M. D. L. C. de Oliveira, *Modeling, Identification and Control of a Quadrotor Aircraft [M.S. thesis]*, Czech Technical University, Prague, Czech Republic, 2011.
- [50] S. Bouabdallah, P. Murrieri, and R. Siegwart, "Design and control of an indoor micro quadrotor," in *Proceeding of the 2004 IEEE International Conference on Robotics and Automation (ICRA '04)*, vol. 5, pp. 4393–4398, May 2004.
- [51] A. Benallegue, A. Mokhtari, and L. Fridman, "Feedback linearization and high order sliding mode observer for a quadrotor UAV," in *Proceedings of the International Workshop on Variable Structure Systems (VSS '06)*, pp. 365–372, Alghero, Italy, June 2006.
- [52] S. Bouabdallah and R. Siegwart, "Full control of a quadrotor," in *Proceedings of the IEEE/RSJ International Conference on Intelligent Robots and Systems (IROS '07)*, pp. 153–158, San Diego, Calif, USA, November 2007.
- [53] C. A. Herda, *Implementation of a quadrotor unmanned arial vehicle [M.S. dissertation]*, California State University, Los Angeles, Calif, USA, 2012.
- [54] J. M. B. Domingues, *Quadrotor prototype [M. S. dissertation]*, Instituto Superior Tecnico, Göttingen, Germany, 2009.
- [55] A. Tayebi and S. McGilvray, "Attitude stabilization of a VTOL quadrotor aircraft," *IEEE Transactions on Control Systems Technology*, vol. 14, no. 3, pp. 562–571, 2006.
- [56] N. A. Chaturvedi, A. K. Sanyal, and N. H. McClamroch, "Rigid-body attitude control," *IEEE Control Systems Magazine*, vol. 31, no. 3, pp. 30–51, 2011.
- [57] V. Mistler, A. Benallegue, and N. K. M'Sirdi, "Exact linearization and noninteracting control of a 4 rotors helicopter via dynamic feedback," in *Proceedings of the 10th IEEE International Workshop on Robot and Human Communication*, pp. 586–593, Paris, France, September 2001.
- [58] J. P. How, B. Bethke, A. Frank, D. Dale, and J. Vian, "Real-time indoor autonomous vehicle test environment," *IEEE Control Systems Magazine*, vol. 28, no. 2, pp. 51–64, 2008.
- [59] M. J. Stepaniak, *A quadrotor sensor platform [Ph.D. dissertation]*, Ohio University, Athens, Ohio, USA, 2008.
- [60] A. Nanjangud, "Simultaneous low-order control of a nonlinear quadrotor model at four equilibria," in *Proceedings of the IEEE Conference on Decision and Control*, pp. 2914–2919, Florence, Italy, December 2013.
- [61] R. K. Agarwal, *Recent Advances in Aircraft Technology*, InTech, Rijeka, Croatia, 2012.
- [62] G. M. Hoffmann, H. M. Huang, S. L. Waslander, and C. J. Tomlin, "Quadrotor helicopter flight dynamics and control-theory and experiment," in *Proceedings of the AIAA Guidance, Navigation and Control Conference and Exhibit*, p. 6461, Hilton Head, SC, USA, 2007.
- [63] P. Pounds, R. Mahony, J. Gresham, P. Corke, and J. Roberts, "Towards dynamically favourable quad-rotor aerial robots," in *Proceedings of the Australasian Conference on Robotics and Automation*, Canberra, Australia, December 2004.
- [64] G. M. Hoffmann, S. L. Waslander, and C. J. Tomlin, "Quadrotor helicopter trajectory tracking control," in *Proceedings of the AIAA Guidance, Navigation and Control Conference and Exhibit*, Honolulu, Hawaii, USA, August 2008.
- [65] G. M. Hoffmann, H. Huang, S. L. Waslander, and C. J. Tomlin, "Precision flight control for a multi-vehicle quadrotor helicopter testbed," *Control Engineering Practice*, vol. 19, no. 9, pp. 1023–1036, 2011.
- [66] P. Pounds, R. Mahony, and P. Corke, "Modelling and control of a quadRotor robot," in *Proceedings to International Conference on Robotics and Automation*, Auckland, New Zealand, 2006.
- [67] R. W. Prouty, *Helicopter Performance, Stability and Control*, Krieger, Melbourne, Fla, USA, 1995.
- [68] J. Seddon, *Basic Helicopter Aerodynamics*, BSP, London, UK, 1990.
- [69] J. G. Leishman, *Principles of Helicopter Aerodynamics*, Cambridge University Press, London, UK, 2nd edition, 2006.
- [70] R. Zawiski and M. Blachuta, "Dynamics and optimal control of quadrotor platform," in *Proceedings of the AIAA Guidance, Navigation, and Control Conference*, AIAA 2012-4915, Minneapolis, Minn, USA, August 2012.
- [71] S. Bouabdallah, *Design and control of quadrotors with application to autonomous flying [M.S. thesis]*, Université Abou Bekr Belkaid Tlemcen, Tlemcen, Algeria, 2007.
- [72] C. Powers, D. Mellinger, and A. Kushleyev, "Influence of aerodynamics and proximity effects in quadrotor flight," in *Proceedings of the International Symposium on Experimental Robotics*, pp. 17–21, Quebec, Canada, 2012.
- [73] N. Guenard, T. Hamel, and L. Eck, "Control laws for the tele operation of an unmanned aerial vehicle known as an X4-flyer," in *Proceeding of the IEEE/RSJ International Conference on Intelligent Robots and Systems (IROS'06)*, pp. 3249–3254, Beijing, China, October 2006.
- [74] W. Johnson, *Helicopter Theory*, Dover, New York, NY, USA, 1980.

- [75] L. Ljung, "Perspectives on system identification," *Journal of Intelligent and Robotic Systems*, no. 74, pp. 129–145, 2014.
- [76] M. Gevers, "A personal view of the development of system identification," *IEEE Control Systems Magazine*, vol. 26, no. 6, pp. 93–105, 2006.
- [77] M. Bergamasco, "Identification of linear models for the dynamics of a hovering quadrotor," *IEEE Transactions on Control Systems Technology*, vol. 22, no. 5, pp. 1696–1707, 2014.
- [78] L. K. Burkamshaw, *Towards a low-cost quadrotor research platform [M.S. thesis]*, Naval Postgraduate School, Monterey, Calif, USA, 2010.
- [79] D. Sonntag, *A study of quadrotor modeling [M. S. dissertation]*, Linköpings Universitet, Linköping, Sweden, 2011.
- [80] L. Derafa, T. Madani, and A. Benallegue, "Dynamic modelling and experimental identification of four rotors helicopter parameters," in *Proceedings of the IEEE International Conference on Industrial Technology (ICIT '06)*, pp. 1834–1839, Mumbai, India, December 2006.
- [81] P. Pounds, R. Mahony, and P. Corke, "System identification and control of an aerobot drive system," in *Proceedings of the Information, Decision and Control Conference (IDC '07)*, pp. 154–159, Adelaide, Australia, February 2007.
- [82] S. Bouabdallah, P. Murrieri, and R. Siegwart, "Towards autonomous indoor micro VTOL," *Autonomous Robots*, vol. 18, no. 2, pp. 171–183, 2005.
- [83] Y. Naidoo, R. Stopforth, and G. Bright, "Quad-rotor unmanned aerial vehicle helicopter modeling and control," *International Journal of Advanced Robotic Systems*, vol. 8, no. 4, pp. 139–149, 2011.
- [84] L. Derafa, T. Madani, and A. Benallegue, "Dynamic modelling and experimental identification of four rotors helicopter parameters," in *Proceedings of the IEEE International Conference on Industrial Technology (ICIT '06)*, pp. 1834–1839, December 2006.
- [85] O. Falkenberg, J. Witt, U. Pilz, U. Weltin, and H. Werner, "Model identification and H_∞ control for MAV's," in *Proceedings of the International Conference on Intelligent Robotics and Applications*, pp. 460–471, Montreal, Canada, 2012.
- [86] G. Gremillion, "System identification of a quadrotor micro air vehicle," in *Proceedings of the AIAA Atmospheric Flight Mechanics Conference*, p. 7644, Toronto, Canada, 2010.
- [87] W. Wei, "Frequency-domain system identification and simulation of a quadrotor controller," in *Proceedings of the AIAA Modeling and Simulation Technologies Conference*, pp. 1834–1839, National Harbor, Maryland, Md, USA, 2014.
- [88] N. Abas, A. Legowo, and R. Akmeliawati, "Parameter identification of an autonomous quadrotor," in *Proceeding of the 4th International Conference on Mechatronics (ICOM '11)*, pp. 1–8, Kuala Lumpur, Malaysia, May 2011.
- [89] L. L. Liu, *Research on the modeling and control to a quadrotor helicopter simulator [M.S. thesis]*, Central South University, Changsha, China, 2009.
- [90] Q. L. Luo, *Application of RBF-ARX model-based predictive control on quad-rotor helicopter simulator [M. S. dissertation]*, Central South University, Changsha, China, 2012, (Chinese).
- [91] S. Yin, X. W. Li, H. J. Gao, and O. Kaynak, "Data-based techniques focused on modern industry: an overview," *IEEE Transactions on Industrial Electronics*, no. 99, pp. 1–11, 2014.
- [92] S. Yin, S. X. Ding, X. C. Xie, and H. Luo, "A review on basic data-driven approaches for industrial process monitoring," *IEEE Transactions on Industrial Electronics*, vol. 61, no. 11, pp. 6418–6428, 2014.
- [93] S. Yin, S. X. Ding, A. Haghani, H. Hao, and P. Zhang, "A comparison study of basic data-driven fault diagnosis and process monitoring methods on the benchmark Tennessee Eastman process," *Journal of Process Control*, vol. 22, no. 9, pp. 1567–1581, 2012.
- [94] S. Yin, G. Wang, and H. R. Karimi, "Data-driven design of robust fault detection system for wind turbines," *Journal of Mechatronics*, vol. 24, no. 4, pp. 298–306, 2014.
- [95] S. Yin, S. X. Ding, A. H. A. Sari, and H. Hao, "Data-driven monitoring for stochastic systems and its application on batch process," *International Journal of Systems Science*, vol. 44, no. 7, pp. 1366–1376, 2013.
- [96] S. Yin, H. Luo, and S. X. Ding, "Real-time implementation of fault-tolerant control systems with performance optimization," *IEEE Transactions on Industrial Electronics*, vol. 61, no. 5, pp. 2402–2411, 2014.
- [97] W. C. Sun, H. J. Gao, and O. Kaynak, "Adaptive backstepping control for active suspension systems with hard constraints," *IEEE Transactions on Mechatronics*, vol. 18, no. 3, pp. 1072–1079, 2013.
- [98] W. C. Sun, Z. L. Zhao, and H. J. Gao, "Saturated adaptive robust control for active suspension systems," *IEEE Transactions on Industrial Electronics*, vol. 60, no. 9, pp. 3889–3896, 2013.

